

Thermal-Hydraulic Characterization and Numerical Modelling with RELAP5 Code of ATHENA Secondary Loop

Tommaso Del Moro,^{a*} Fabio Giannetti,^a Mariano Tarantino,^b
Pierdomenico Lorusso,^c Marco Caramello,^d Damiano Vitale Di Maio,^e and
Marin Constantin^f

^a *Sapienza University of Rome, Department of Astronautical, Electrical and Energy Engineering, Rome, Italy*

^b *ENEA, Department for Fusion and Technology for Nuclear Safety and Security, Camugnano (BO), Italy*

^c *ENEA, Department for Fusion and Technology for Nuclear Safety and Security, Frascati (RM), Italy*

^d *Ansaldo Nucleare S.p.A., Genova, Italy*

^e *S.R.S. Servizi di Ricerche e Sviluppo S.r.l., Rome, Italy*

^f *RATEN ICN, Institute for Nuclear Research, Pitesti, Romania*

*E-mail: tommaso.delmoro@uniroma1.it

Thermal-Hydraulic Characterization and Numerical Modelling with RELAP5 Code of ATHENA Secondary Loop

Among the envisaged experimental infrastructures supporting ALFRED reactor development, FALCON consortium identified ATHENA as one of the facilities to address the pool thermal-hydraulic challenges and demonstrate the feasibility of the revised ALFRED configuration, along with the thermal-hydraulic performances of its main components. ATHENA is a large pool-type lead-cooled multi-purpose experimental facility featuring a large size vessel (3.2 m diameter, 10 m in height), conceived to host almost 800 tons of lead to test ALFRED relevant scaled components. The test section to be installed in the main vessel includes an electrically heated core simulator, made of 7 FAs, which delivers to the primary coolant a nominal thermal power of 2210 kW, a main coolant pump for lead circulation and a counter-current shell and tubes main heat exchanger, which tube bundle is fed by pressurized water by a dedicated secondary circuit. In this work the numerical model of ATHENA is presented, along with the thermal-hydraulic characterization of the facility using the system code RELAP5/Mod3.3, properly modified to include the thermo-physical properties of heavy liquid metals. After the characterization of the steady state representative of the Stage 3 foreseen for the ALFRED staged approach, results of a numerical sensitivity analysis aimed at defining the most suitable procedure for the shutdown transient of the facility are presented.

Keywords: Lead Fast Reactors; ALFRED; ATHENA; heavy liquid metals; SYS-TH analysis

I. INTRODUCTION

In the framework of the Gen-IV^{[1][2]} nuclear power plants development, the Heavy Liquid Metal (HLM)-cooled fast reactors^[3] represent one of the most promising technologies for achieving the Gen IV standards of safety and reliability required for civil applications of nuclear power. In support to the R&D activities related to the design of the Lead Fast Reactor (LFR) European demonstrator ALFRED (Advanced Lead Fast Reactor European Demonstrator)^{[4][5][6]} in its revised configuration^[7], a new prototypical experimental facility, named ATHENA^[8] (Advanced Thermo-Hydraulics Experiment for Nuclear Application) is currently under design thanks to the joint effort between ANSALDO NUCLEARE and ENEA, in collaboration with the RATEN ICN.

ATHENA facility is part of the experimental platform to be realized in Romania, which is needed for the licensing process in order to understand the main thermal-hydraulic phenomena involved in a pool system, as well as to qualify the materials, the operational stages of ALFRED, and to validate computer tools^{[9][10]}. ATHENA is dedicated to developing the technologies based on HLMS through (i) the testing of systems and components in relevant scale representative of the LFRs, (ii) the investigation of thermal-hydraulic phenomena as operational and accidental regimes, natural circulation and stratification of the coolant, and (iii) the evaluation of the chemistry control capability in large pool systems. The new experimental platform will complement the activities ongoing or performed at ENEA experimental fleet^[11], which has been involved in several European Commission (EC) programs to investigate the HLMS behavior and to support the technological development of the LFRs.

This work aims at providing a description of ATHENA facility, illustrating in detail the lead flow path inside the main vessel, as well as the water secondary circuit. The numerical model of ATHENA facility obtained by the thermal-hydraulic system code RELAP5/Mod3.3^{[12]-[16]} is presented, and a complete steady state characterization is

performed considering the lead thermal cycles representative of the Stage 3 operation foreseen within the staged approach^[17] defined for the ALFRED reactor, i.e., 400-520°C as inlet-outlet temperatures from the Core Simulator (CS). Starting from the nominal steady state, the shutdown transients is analyzed, consisting in the assessment of the behavior of the facility during the operational shutdown phase, in which the CS is switched off following the power curve provided for the operation of the component. The Main Circulation Pump (MCP) is assumed to elaborate the nominal flow rate during the steady state to avoid the stagnation and freezing of the lead in the pool.

II. ATHENA FACILITY DESCRIPTION

ATHENA is a large multipurpose pool-type facility, having a power installed of 2210 kW, and using pure lead as primary coolant and pressurized water as secondary cooling fluid. The large scale of the main vessel (3.2 m diameter and 10 m in height) allows to test the LFR components in relevant scale, as well as to reproduce in a reliable way the main phenomena occurring in a large lead-cooled pool-type reactor. The facility will be operated to reproduce the lead thermal cycle as intended in ALFRED, following the steps defined in the staged approach. The design of the facility benefits from the previous experience of ENEA, collected during design activities and experimental campaigns performed on the large pool-type facility CIRCE (CIRColazione Eutettico, Eutectic Circulation)^[18] in its HERO (Heavy liquid mEtal – pRessurized water cOoled tube)^{[19][20][21]} and THETIS (Thermal-hydraulic HELical Tubes Innovative System)^{[22][23]} configurations, at ENEA Brasimone Research Centre. The main vessel layout and the P&ID of the secondary loop of the facility are shown in Figure 1 and Figure 2.

II.A. Primary System

The test section contained in the ATHENA main vessel is composed by the main electrical heater reproducing the ALFRED fuel assembly, the pumping system^{[24][25]} to be installed in the hot leg exiting from the CS, and the Main Heat eXchanger (MHX)^[26] fed by lead provided by the pump. The internals are constituted by the suction duct connected to the heater housing duct, a riser that contains the main pump and connects the heater outlet to the hot pool, which delivers the lead to the MHX, and a dead volume^[27] which hosts heater cables and instrumentation connections. During normal operation, lead is heated by the CS at the bottom part of the main vessel, flows upward and it is pulled by the pump in the hot pool. Then, it enters the MHX shell side and moves downward in counter current with respect to the secondary fluid and goes into the cold pool. To avoid thermal stratification, the cold lead is diverted into a descendent annulus between the main vessel and the barrel, before entering the CS again. The flow path is qualitatively shown in Figure 1.

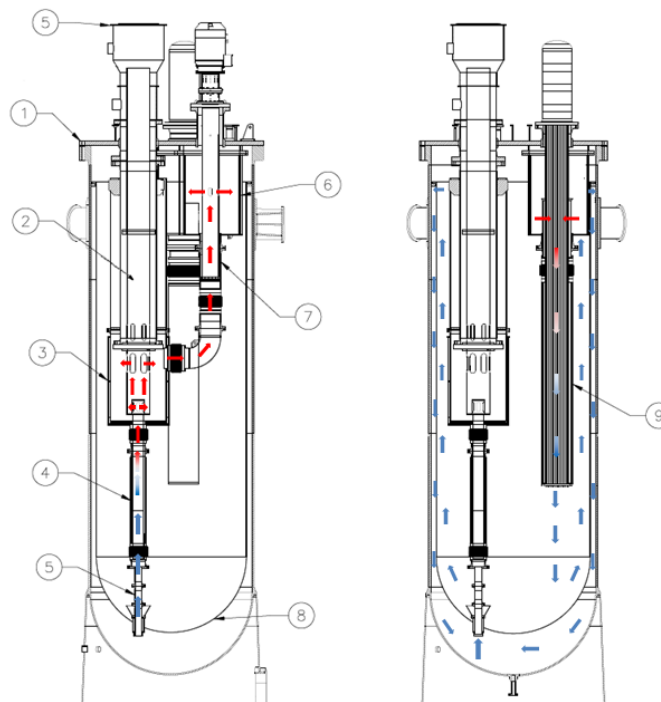


Figure 1. ATHENA Main Vessel layout and primary coolant flow path (legend: (1) Main Vessel, (2) Dead Volume, (3) Fitting Volume, (4) Core Simulator, (5) Feeding Conduit, (6) Separator, (7) Main Circulation Pump, (8) Barrel, (9) Main Heat Exchanger)

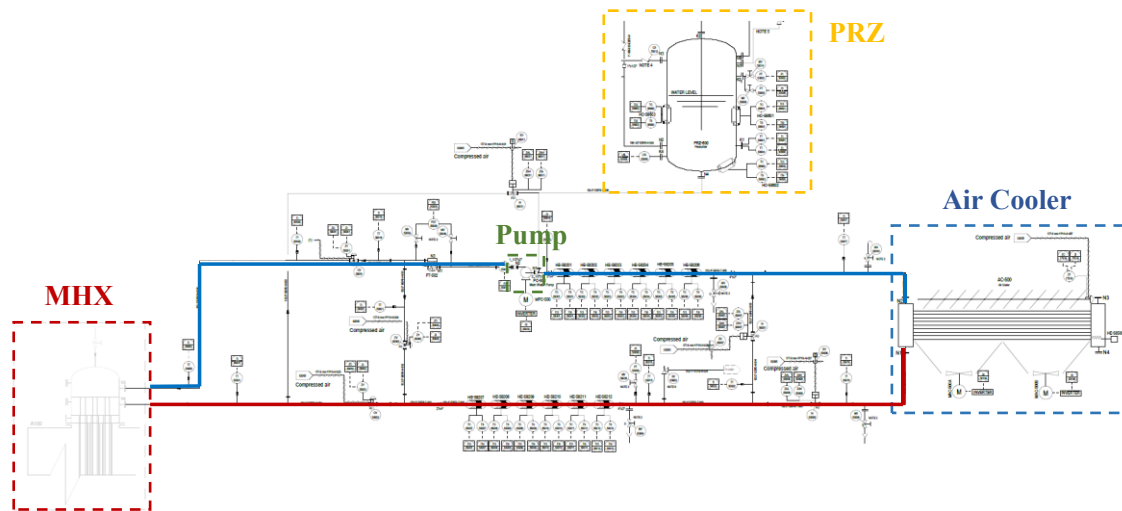


Figure 2. Conceptual scheme of the ATHENA facility secondary system

II.A.1. Core Simulator

The main test section of ATHENA is the Core Simulator, which aims to characterize an average Fuel Assembly (FA) of ALFRED reactor from a thermal-hydraulic point of view, both in forced and in natural circulation, including the inter-wrapper flow and the thermal coupling among FAs.

The CS configuration that is considered as the most suitable for the purpose of the facility is characterized by 127 pins. A cross section is shown in Figure 3, where the wrappers subdivision is highlighted: a hexagonal central one (in blue) with 61 pins (60 active + 1 dummy element) is surrounded by 6 smaller polygonal wrappers (in blue) with 11 pins each. Around them, a polygonal shroud (in green) is installed to limit lead bypass around the assemblies. The hexagonal and trapezoidal wrappers, and the external shroud are part of the CS assembly. The external pipe surrounding the shroud is a 10'' Sch. 40. The six trapezoidal wrappers surrounding the central one aim at reproducing the effect of the adjacent FAs in the reactor core.

The active length of the pin is 810 mm, with a total length of in lead of 3115 mm from the bottom grid – which maintains the pins in the correct position – to the flange that isolates the lead from the dead volume through a sealing mechanism.

Together with the bottom grid, an upper grid and 3 spacer grids are used to keep in position the entire pin bundle. In Figure 4 a preliminary design of the spacer grids for the different assemblies is shown. Other parameters from the engineering design are reported in Table I.

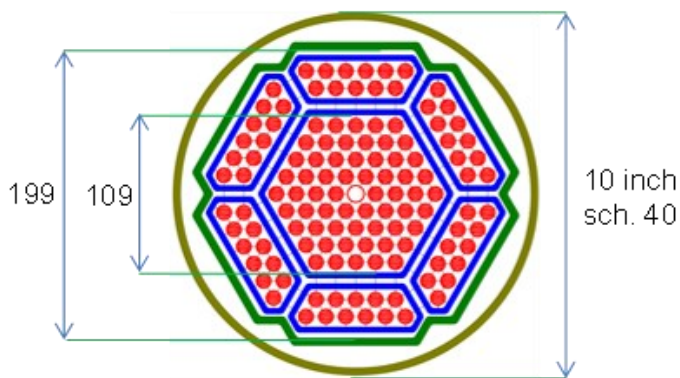


Figure 3. Schematic layout of the ATHENA Fuel Assembly

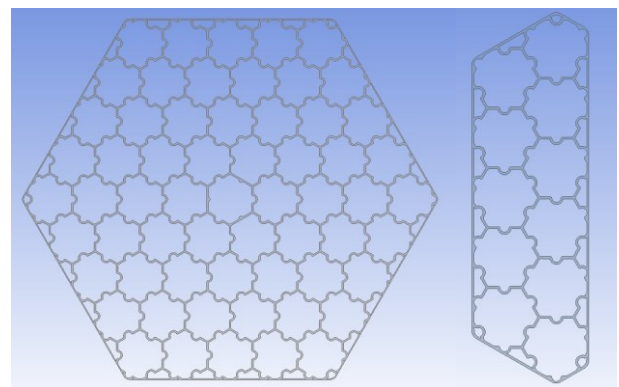


Figure 4. Schematic layout of the spacer grids

Parameter	Unit	Value
<i>Pin diameter</i>	mm	10.5
<i>Central pin Diameter</i>	mm	12.0
<i>Pitch</i>	mm	13.6
<i>Pitch to Diameter ratio</i>	----	1.29
<i>Number of pins</i>	----	126 (active)+1 (dummy)
<i>Active length</i>	mm	810.0
<i>Pin total length</i>	mm	8550.0
<i>Central wrapper hexagonal key</i>	mm	109.0
<i>Shroud hexagonal key</i>	mm	199.0
<i>Total power</i>	MW	2.21
<i>Linear power</i>	kW/m	21.65
<i>Max wall heat flux</i>	kW/m ²	656.0
<i>Number of FAs</i>	-	1 (61 pins) + 6 (11 pins)

Table I. CS geometry and power of the pins

II.A.2. Main Circulation Pump

The lead pump in ATHENA is a vertical axial type and it is installed in the cover of the main vessel, as the other test sections. The suction is from the lower part of the component, while the discharge occurs through six lateral buttonholes towards the hot pool. The main MCP design data are reported in Table II, while the drawing is presented in Figure 5.

Parameter	Unit	Value
<i>Working fluid</i>	----	Lead
<i>Working temperature</i>	°C	480-520
<i>Nominal flow rate</i>	m ³ /h	45
<i>Maximum flow rate</i>	m ³ /h	65
<i>Pressure head</i>	MPa	0.2
<i>Type</i>	----	Axial
<i>Shroud external diameter</i>	mm	330
<i>Shroud thickness</i>	mm	5
<i>Total length (beneath the flange)</i>	mm	3020

Table II. ATHENA MCP design data^[25]

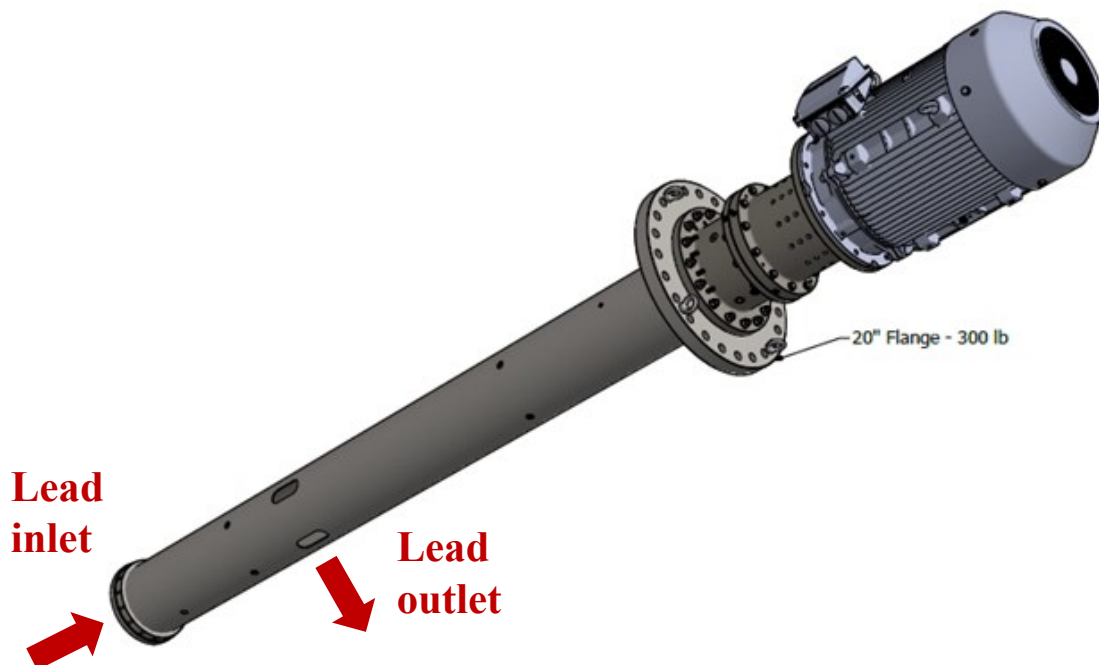


Figure 5. ATHENA Main Circulation Pump

II.A.3. Main Heat Exchanger

The configuration adopted for the ATHENA Main Heat eXchanger (MHX) is the concept with double wall Bayonet Tubes (BTs). The calculation reported in Ref. [26] has shown that the tube bundle is composed of 91 BTs with an active length (in lead) of 3 m, that is a requirement for maintaining the same difference in height between the thermal barycenters of the heat source (CS) and the heat sink (MHX) compared to ALFRED.

The bayonet tubes are composed of three coaxial tubes (Figure 6): the innermost acts as a downcomer, and the riser is realized between the first and the second tubes. The gap between the second and the third tubes is filled with pressurized helium at 0.5 MPa, acting as an insulator and allowing the BTs to withstand to huge thermal gradients without relevant thermal stresses on the materials.

The BTs are arranged in a cylindrical array (Figure 7) with a minimum pitch-to-diameter ratio of 1.3, and the bundle is surrounded by a cylindrical double wall shell that separates the component from the pool. The details are reported in Table III and Table IV. The technical drawing is shown in Figure 8.

Parameter	Unit	Value
<i>Number of bayonet tubes</i>	----	91
<i>Tube bundle active length</i>	mm	3000
<i>Pitch to Diameter ratio</i>	----	1.3
<i>Pitch geometry</i>	----	Cylindrical
<i>Bayonet tube geometry</i>	----	3 coaxial tubes
<i>Shell inner diameter</i>	mm	499

Table III. ATHENA MHX tube bundle configuration

Parameter	I.D. [mm]	O.D. [mm]	Thick. [mm]	Size
<i>First tube</i>	22.90	25.40	1.25	1" BWG 18
<i>Second tube</i>	28.45	31.75	1.65	1 ¼" BWG 16
<i>Third tube</i>	33.15	34.93	0.89	1 3/8" BWG 20

Table IV. ATHENA MHX tubes dimensions

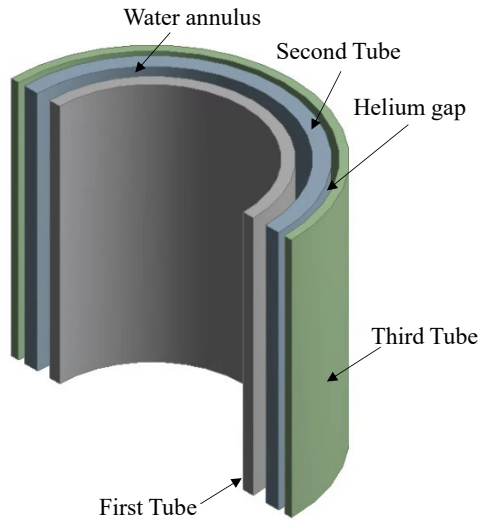


Figure 6. Internal view of the bayonet tube

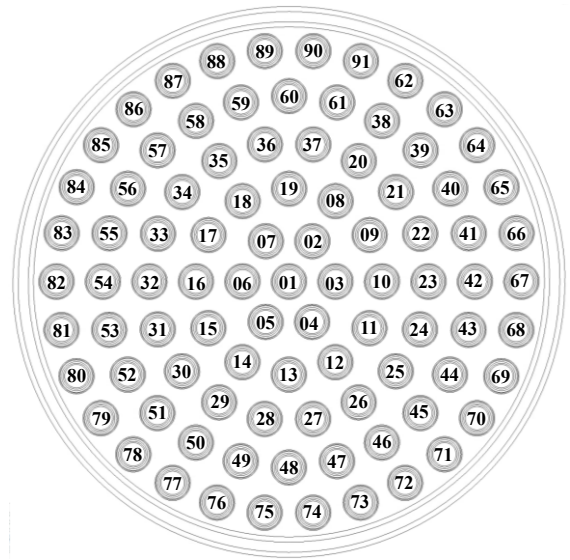


Figure 7. Cross section view of the MHX tube bundle

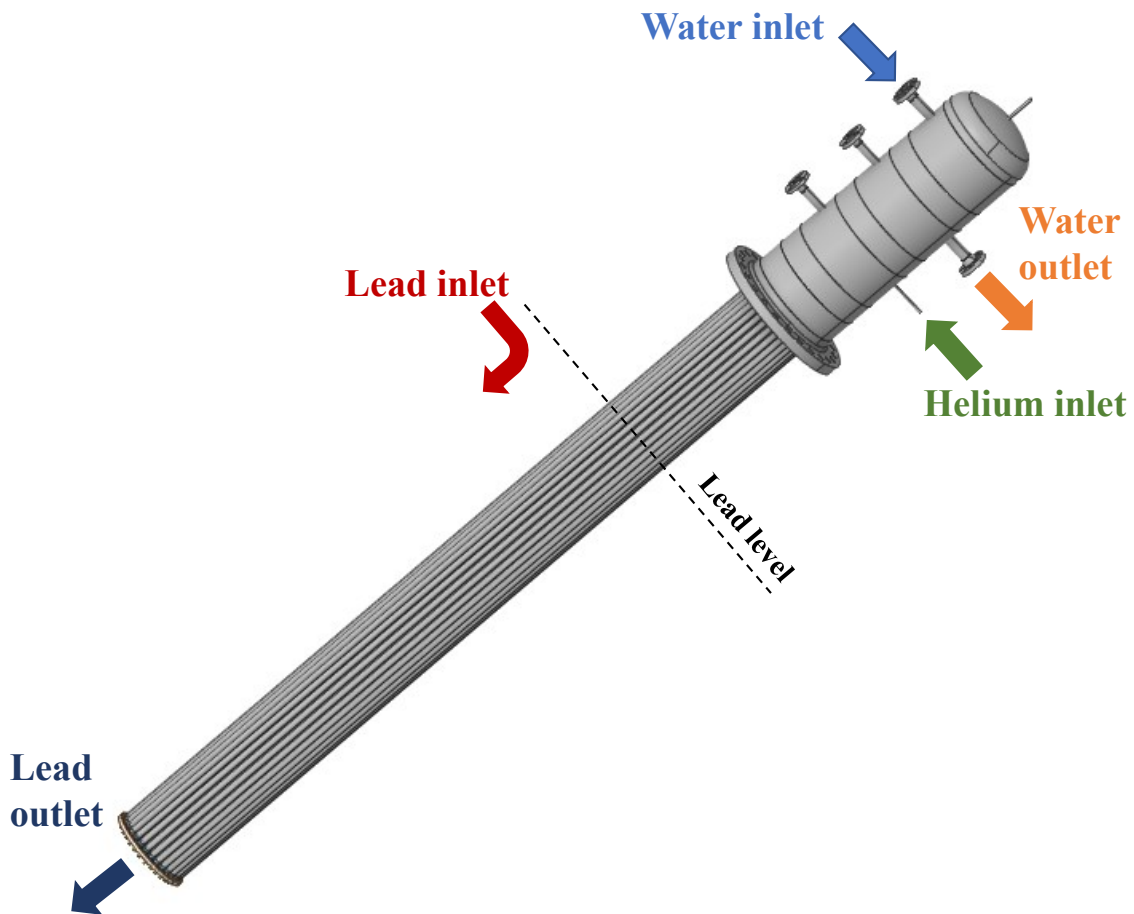


Figure 8. ATHENA MHX

II.B. Secondary System

The primary and secondary systems are thermally coupled through the MHX. The tube side of the MHX is fed by a dedicated loop, from which the cold water is collected in the inlet manifold in the upper part of the MHX, it flows downward in the slave tube that acts as a downcomer, inverts its direction at the bottom of the BTs, moves upward in the annular riser where it is heated by the lead, and, then, it exits in the outlet manifold in the upper part of the MHX. Both the collectors are located outside the main vessel, above the coupling flange.

The secondary loop is composed of:

1. 2” main lines, acting as hot and cold legs;
2. a pump, assuring the water circulation along the loop;
3. an electrical heater, that works in the start-up phase only (the MHX is bypassed in that case). In this work, this heater is not involved in any transient;
4. air coolers (AC), consisting in a horizontal tube bundle from which the power is removed by air blown by fans. The heat transfer is enhanced by fins on the outer surface of the tubes;
5. a pressurizer (PRZ), that acts as an expansion tank and a pressure regulator for the system by injecting (discharging) nitrogen in (from) the cover gas region;
6. MHX and AC bypass lines, that are closed in normal operation, and they works only if one of the two components has to be bypassed.
7. the venting line that connects the MHX directly to the PRZ during the shutdown of the facility and the following emptying of the MHX;

8. a system of valves that serves to isolate specific components of the loop and to regulate the injection or discharge of the PRZ and main vessel cover gas regions;
9. an auxiliary system to provide the cover gas to the lead tanks and to the PRZ.

II.C. ATHENA operating condition

ATHENA facility aims at reproducing the main phenomena governing the thermal-hydraulics of a large pool-type system. Since ALFRED is foreseen to operate following a staged approach, ATHENA will reproduce the thermal-hydraulic conditions of the so called “Stage 2” and “Stage 3”. While in ALFRED reactor, the stages consist in gradually increase the thermal power and the maximum temperature, in ATHENA the reproduction of the stages is realized by increasing the maximum temperature only while keeping constant the electrical power provided to the CS, by properly adjusting the lead mass flow rate. The comparison between the two stages is reported in Table V.

Parameter	Unit	Stage 2	Stage 3
<i>Total power</i>	MW	2.21	2.21
<i>Pb temperature at CS inlet</i>	°C	400.0	400.0
<i>Pb temperature at CS outlet</i>	°C	480.0	520.0
<i>Lead mass flow rate</i>	kg/s	189.3	126.5
<i>Water temperature at MHX inlet</i>	°C	110.0	110.0
<i>Water temperature at MHX outlet</i>	°C	160.0	200.0
<i>Water mass flow rate</i>	kg/s	10.34	5.67
<i>Water pressure (in the PRZ)</i>	MPa	1.20	2.50

Table V. Thermal-hydraulic characterization of ATHENA

III. ATHENA NUMERICAL ANALYSIS BY RELAP5/MOD3.3 CODE

III.A. Description of the Model

Primary and secondary systems have been modelled through two independent systems thermally coupled through a heat structure. The adopted nodalization is based on the so called “sliced modelling approach”^[28], that consists in discretize components at the same absolute height with mesh having the same length. For example, the fluid elements that compose the MHX have the same length for the entire active length. The validity of this approach has been also qualified in a benchmark on CIRCE facility^{[29][30]}. The average mesh size is 0.15 m with a maximum length difference between two adjacent meshes of 25%. The first numbers of the hydrodynamic components reference to a specific system are:

- “1XX” for primary side hydrodynamic components;
- “2XX” for secondary side components of the loop;
- “3XX” for the pressurizer system and surge line;
- “4XX” for the venting line and bypass lines;
- “5XX” for air side of the AC.

The version of RELAP5/Mod3.3 used in this work has been modified to implement the HLMs (i.e., lead, lead-bismuth eutectic, lithium-lead) thermophysical properties^[31] and the related heat transfer correlations^{[32][33]}. The code with such implementations has been used in post-test analysis and numerical benchmark exercises^{[29][34]}, proving its reliability in simulating the main phenomena occurring during the experiments involving HLMs, along with a satisfactory prediction of the trends of the main operating parameters.

III.A.1. Primary Side Hydraulic Components

The nodalization of the primary system is reported in Figure 9.

The Feeding Conduit (FC) has been modelled with the PIPE 142, from which the flow enters the CS, and it is divided between two pipe components that simulate the fluid near the pins and the bypass region, respectively. The first is then divided between the Central Assembly (PIPE 150) and the Lateral Assemblies (PIPE 162). In this region, the 810 mm active length is contained. At the CS outlet, lead goes into the fitting volume (PIPE 170), then flows into the riser (PIPE 172) before entering the MCP and the hot pool (PIPE 185). From the hot pool, lead flows downward through the MHX active part (103) and then in the shell part without the bayonet tubes. At the outlet of the MHX, lead exits in the cold pool inside the barrel (pipes from 112 to 134), rises again up to the free level and flows through buttonholes in the main vessel region (PIPE 140). At the bottom of this region, the fluid enters again the Feeding Conduit.

The discretization approach of the cold pool with three vertical parallel pipes (from 112 to 134) has been qualified against experimental data from CIRCE facility in Ref. [28][29][30], where a good agreement with experimental data is shown in transients where details on the pool are not required. This technique allows shorter simulation time that is useful for long transient simulations. For the purposes of this work, the three-pipes nodalization has been adopted since focus on the pool is not required.

III.A.2. Secondary Side Hydraulic Components

The nodalization of the secondary side is shown in Figure 10. Water in the secondary side enters the MHX from the upper collector, flows inside the bayonet tubes and it is collected in the hot water plenum. Hot water goes to the AC (PIPE 222 to 226) through the hot leg (209 to 219) where it is cooled down by air (502). Then, cold water

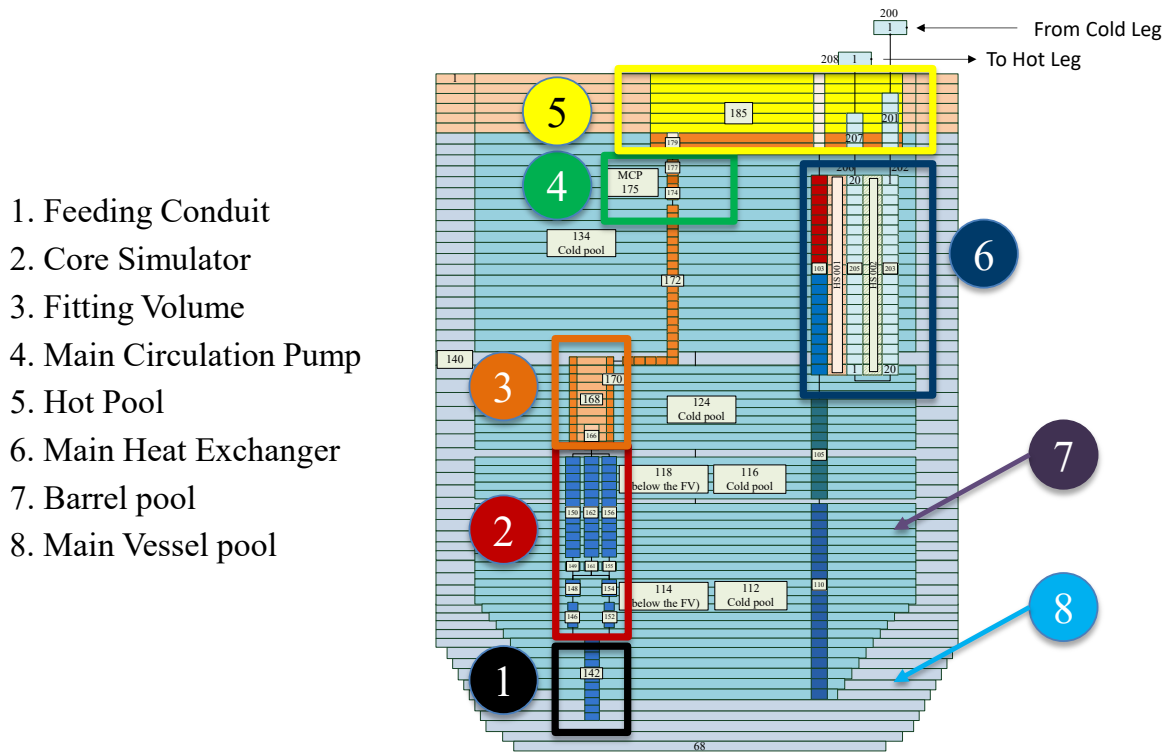
goes back to the MHX through the cold leg (230 to 258), where the surge line inlet and the pump are installed.

III.A.3. Heat Structures

The main heat structures are:

1. the CS:
 - a. 150-0 is the central assembly pins (with power generation);
 - b. 156-0 is the external assembly pins (with power generation);
 - c. 162-0 and 162-1 are the thickness of the central and polygonal wrappers.
2. the MHX is modelled through the structure 001-0, which simulates the thicknesses of the second and third tubes and the helium gap
3. the AC (003-0) models the heat transfer to the air, considering the fins through a multiplying factor of the heat transfer coefficient. This approach is not appropriate for considering the thermal inertia of the fins, but for the purposes of this paper it is considered acceptable.

Other heat structures inside the main vessel are added to consider the heat transfer inside the pool through the internals, and a rockwool insulator is considered to account for the heat losses of the main vessel, as well as of the secondary loop. These heat structures are not represented in the figures.



1. Feeding Conduit
2. Core Simulator
3. Fitting Volume
4. Main Circulation Pump
5. Hot Pool
6. Main Heat Exchanger
7. Barrel pool
8. Main Vessel pool

Figure 9. ATHENA pool nodalization

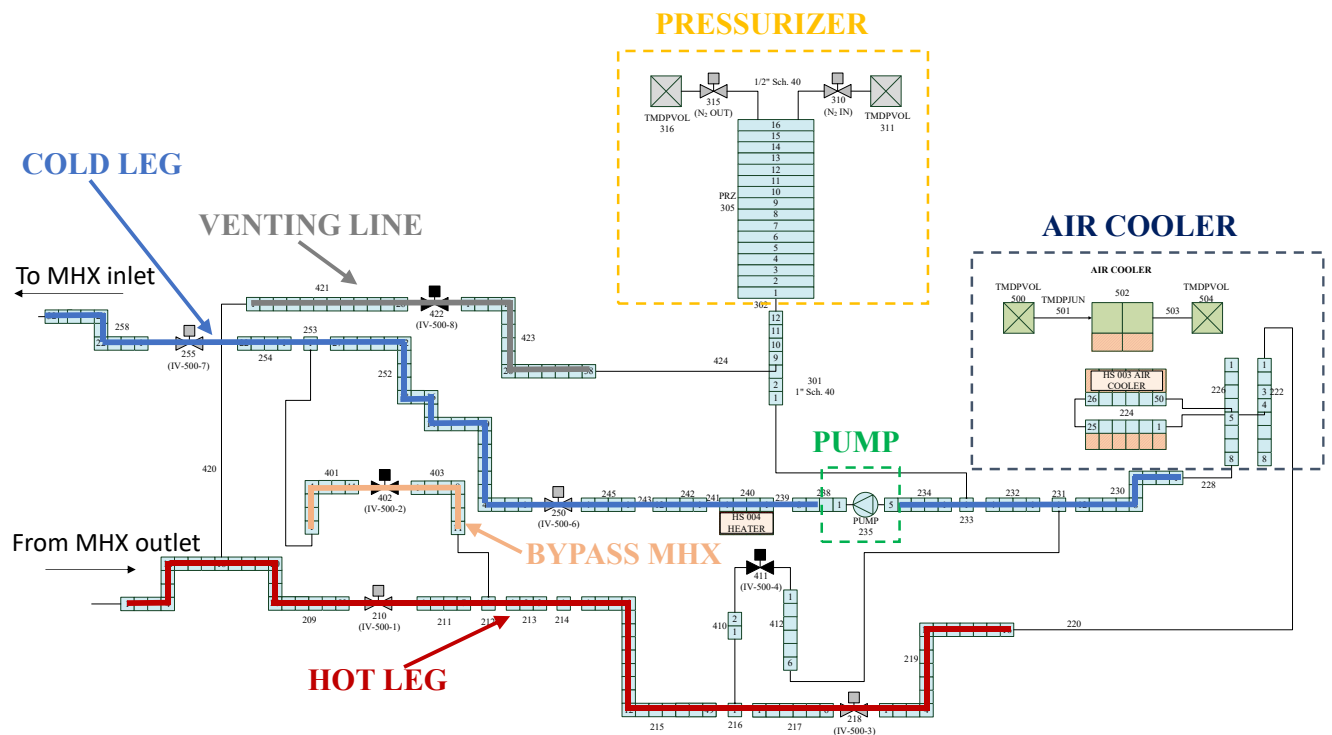


Figure 10. ATHENA secondary loop nodalization

III.B. Steady State Characterization

In this section, the steady state characterization of ATHENA facility is presented for the for the Stage 3 operation. The steady state has been reached in the simulation through a 5000 s of “null-transient” with the boundary conditions reported in Table VI. Mass flow rates are not properly boundary conditions, but the pumps are regulated through a control system.

Parameter	Unit	Stage 3
<i>Total power</i>	MW	2.21
<i>Pb initial temperature</i>	°C	400.0
<i>Lead mass flow rate</i>	kg/s	126.5
<i>Cover gas pressure</i>	MPa	0.135
<i>Water initial temperature</i>	°C	110.0
<i>Water mass flow rate</i>	kg/s	5.67
<i>Water pressure</i>	MPa	2.50
<i>Environmental temperature</i>	°C	10.0

Table VI. Boundary conditions

Results of the steady state calculation (see Table VII) show that with the distribution of the mass flow among the central assembly, the lateral assemblies and the bypass, the outlet temperatures from the three regions of the CS are close to each other (~520°C). This distribution agrees with the CFD calculation of Ref. [35], which predicts values of 51%, 47.4% and 1.6% in the above mentioned regions, respectively.

The design conditions for the lead are respected, i.e., cycle 400-520°C and mass flow rate equal to 126.5 kg/s. In these conditions, the foreseen secondary cycle^[26] at 110-200°C at 2.5 MPa is well reproduced, and the subcooling at the outlet of the MHX is about 24°C.

From the 2.21 MW delivered form the CS, only 2.187 MW are removed by the water in the MHX because of the heat losses, that are equal to 23 kW, assuming a heat

transfer coefficient with the environment of $8 \text{ W/m}^2 \text{ K}$. The evaluation of the heat losses is then performed by adding the power exchanged of all the control volumes through the main vessel wall and insulator heat structure. Regarding the secondary side, the heat losses are much lower because of the low temperature of the secondary loop, therefore almost all the power removed from the MHX is exchanged in the AC.

Pressure drops in the CS ($\sim 64.6 \text{ kPa}$) are close to the calculation of Ref. [35], while pressure drops in the MHX are negligible due to the very small velocity in the component ($\sim 0.1 \text{ m/s}$). In the secondary loop, the pressure drop across the MHX is about 14 kPa , which is a very low value compared to the overall loop pressure losses ($\sim 210 \text{ kPa}$). The pressure in the main vessel is kept thanks to the slight pressurization of the cover gas (0.135 MPa), therefore the maximum pressure is reached at the bottom of the vessel because of the static head of the lead, and it is equal to about 1.34 MPa . In the secondary loop, pressure is fixed in the PRZ at 2.5 MPa through the injection and discharge of nitrogen forming the PRZ cover gas to regulate the pressure. Pressure in the MHX is slightly increased because of the pressure drops between the PRZ and the MHX.

Parameter		Unit	Value
Primary side parameters			
<i>Mass flow rates</i>	Γ_{TOT}	kg/s	126.5
	$\Gamma_{Ext.A.}$		64.6 (51.1%)
	$\Gamma_{Cen.A.}$		60.4 (47.7%)
	Γ_{TOT}		1.5 (1.2%)
<i>Temperatures</i>	$T_{in,CS}$	°C	400.6
	$T_{out,Ext.A.}$		520.2
	$T_{out,Cen.A.}$		516.9
	$T_{out,Bypass}$		517.4
	$T_{out,CS}$		518.6
	$T_{in,MHX}$		516.9
	$T_{out,MHX}$		400.5
<i>Powers</i>	CS	kW	2210
	MHX		2187
	Heat losses		23
<i>Absolute pressures</i>	$p_{bottom,pool}$	MPa	1.34
	$p_{cover\ gas}$		0.135
<i>CS pressure drops</i>	Δp	kPa	64.6
Secondary side parameters			
<i>Mass flow rates</i>	Γ_{H_2O}	kg/s	5.67
<i>Temperatures</i>	$T_{in,MHX}$	°C	110.3
	$T_{out,MHX}$		199.2
	$T_{in,AC}$		199.1
	$T_{out,AC}$		110.0
<i>Powers</i>	MHX	kW	2187
	AC		2185
	Heat losses		2
<i>Absolute pressures</i>	p_{MHX}	MPa	2.63
	p_{PRZ}		2.50
<i>Pressure drops</i>	Δp_{MHX}	kPa	14.3
	Δp_{loop}		208.4

Table VII. Steady state characterization

III.C. Transient analysis

The transient analyzed in this paper is the shutdown of the facility: the CS is switched off while the MCP continues to operate in order to keep the circulation of the lead and avoiding the stagnation of the coolant in the pool. After the shutdown of the CS, power is gradually decreased in 22 min following the trend reported in Figure 11 (black curve). After a certain time, the MHX is intercepted and isolated from the secondary loop, so that the removal of power is stopped to avoid the lead freezing. The mass of water contained in the MHX in that moment starts to boil and the steam goes directly to the PRZ through the venting line.

In order to set up the most suitable procedure for the shutdown transient of the facility, two sensitivity analysis have been carried out varying:

1. the time at which the MHX is isolated from the secondary loop;
2. the time of the decreasing of the CS power.

These sensitivity analyses have been performed because of the difficulty in the regulation of the power removed by the secondary side. Preliminary calculations have shown that all the three different control systems tested during the transient fail in controlling the removal of power. The control systems consist in regulate the water mass flow rate in order to:

1. maintain 400 °C at the MHX outlet;
2. keep the power delivered by the lead equal to the power removed by the

$$\text{water, i.e., } (\dot{m} \cdot c_p \cdot \Delta T)_{Pb} = (\dot{m} \cdot c_p \cdot \Delta T)_{H2O};$$

3. apply the normalized trend of the CS power to the mass flow rate.

Calculations have shown that the water temperature increases as the water mass flow rate decreases, and the lead temperature at the MHX outlet decreases as well. When water flow rate decreases below a certain value (about half of the initial value), boiling in

the tubes starts and lead temperature continue to decrease. After few seconds, most of the water is boiled off and lead temperature quickly increase because of the low heat transfer coefficient of the steam. Therefore, the regulation of the power exchanged in the MHX is quite difficult because of the very high logarithmic mean temperature difference between the fluids and the very small thermal inertia of the secondary side, that leads to the early boiling of the water.

The transient scheme in the sensitivity analyses is defined as follows:

1. at $t=0$ min the CS starts to shut down (in the following it is named SoT, Start of Transient);
2. at $t=1$ min (other cases at 3, 6, 10 min) the valve on the bypass line is opened. When the opening is completed (in 2 s), the isolation valves are closed, and the venting line valve is opened. The MHX is isolated from the secondary loop and it is connected directly to the PRZ;
3. at $t=22$ min (other cases at 15, 10 min) the power delivered by the CS is null.

When the steam produced in the MHX goes into the PRZ, it condenses until PRZ reaches saturation conditions, and pressure increases because of the increase of the water level. To compensate the increase of pressure, the PRZ discharge valve is opened at 2.6 MPa and remains opened until pressure drops again below 2.55 MPa.

The main constraints for the operation of the facility during the shutdown phase are the minimum temperature of the lead, that must be above $\sim 350^{\circ}\text{C}$ (23°C margin on the freezing temperature), and the maximum pressure in the secondary loop that must be below the design pressure of the components (4 MPa).

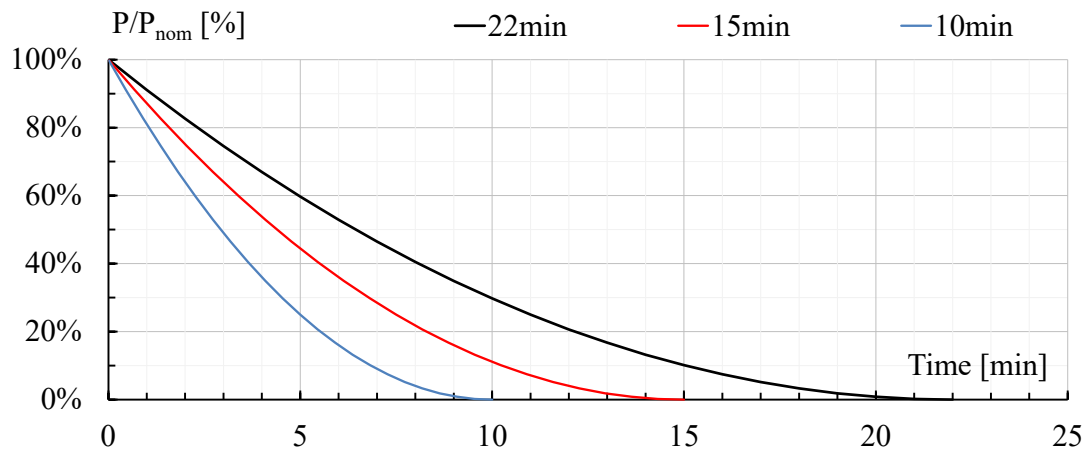


Figure 11. Power trend during Core Simulator shutdown

III.C.1. Sensitivity analysis on the MHX isolation time

Considering the reference power curve for the CS shutdown (22 min), four different times for the MHX isolation have been tested in the sensitivity analysis: it is assumed that the MHX is isolated at 1, 3, 6, and 10 minutes after the SoT. When the isolation valves are closed, the mass flow in the MHX drops to zero, and after ~1 min from the isolation, big oscillations (see Figure 12) occur in the MHX due to the boiling in the MHX and the condensation in the PRZ. However, these oscillations are dumped in ~10 min when a new equilibrium conditions is reached. The amplitude of the oscillations depends on the time after which the MHX is isolated: later is the isolation, smaller are the oscillations because of the reduction of the power delivered by the CS.

Figures 13 and 14 show that boiling starts as soon as the isolation valves are closed. At ~7 min after the isolation the void fraction decreases, meaning that a certain amount of water is flowing inside the MHX, and the presence of water remains for ~4 min. The reason can be addressed to the saturation of the capability of the PRZ in condensing the steam coming from the MHX: the PRZ relief valve opens and the steam/water in the PRZ are discharged (see Figure 15). Therefore, a certain amount of

water remained in the feedwater collector of the MHX flows inside the bayonet tubes, cooling the lead until the discharge stops. At this moment, the water completely boils again (void fraction in Figure 14 increases to 1) and lead temperature increases (Figure 16).

The pressure transient in the PRZ and MHX is shown in Figures 17 and 18. The cases at 1, 3, and 6 min exhibit an increase of pressure ~7 min after the MHX isolation because of the discharge of the not condensed steam from the PRZ, while the case at 10 min does not exhibit significant pressure peaks in the PRZ nor in the MHX. The blue curve (case at 6 min) has a further peak of 3.6 MPa in the MHX, which is close to the design pressure of the components of the secondary loop (4 MPa).

The level in the PRZ increases from the starting value of 1 m to ~2.5 m (see Figure 19) for all the cases analyzed, from which the mass of water is not able anymore to condense the steam and the remaining mass is discharged.

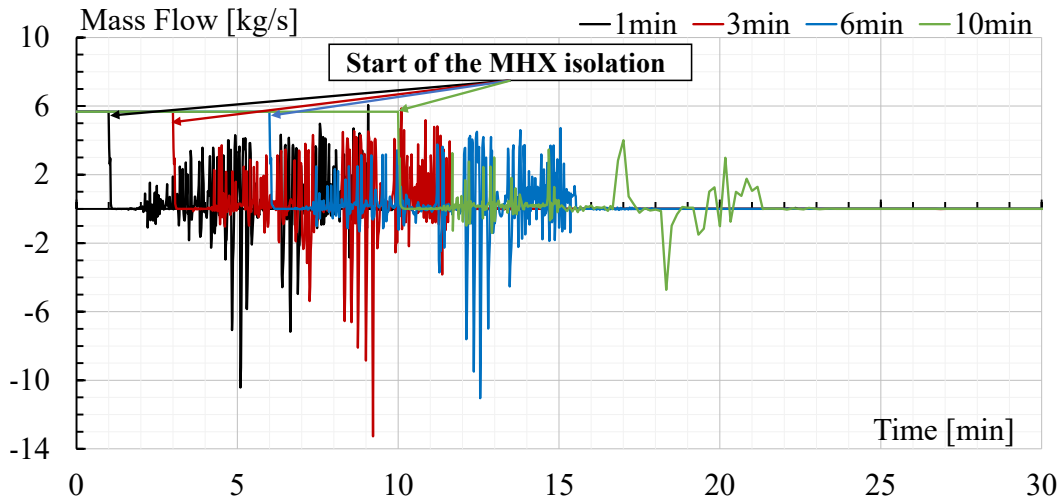


Figure 12. Water mas flow rate trend at different MHX isolation times

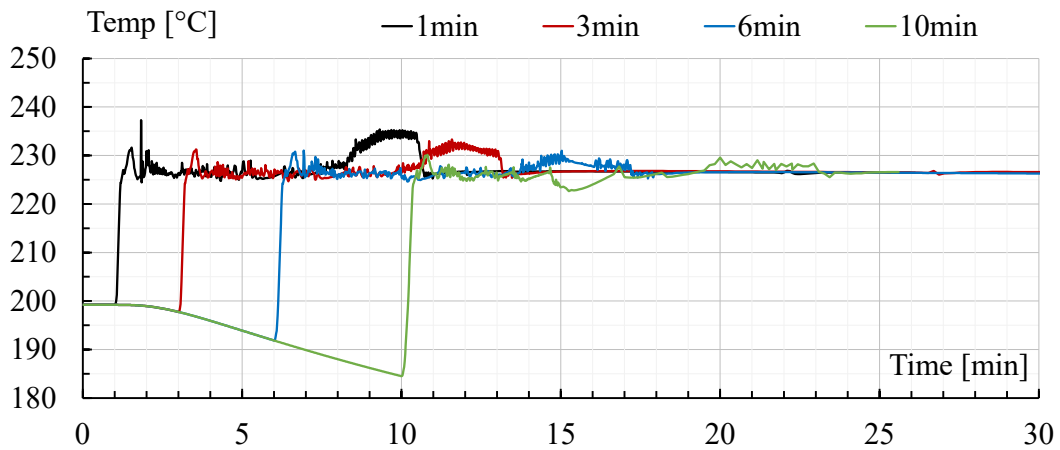


Figure 13. Water temperature trend at MHX outlet at different MHX isolation times

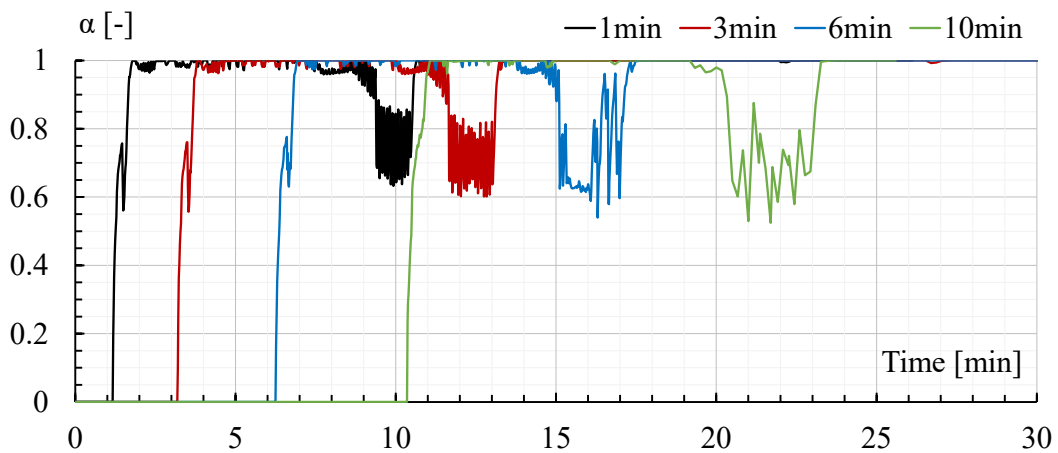


Figure 14. Void fraction trend at MHX outlet with different MHX isolation times

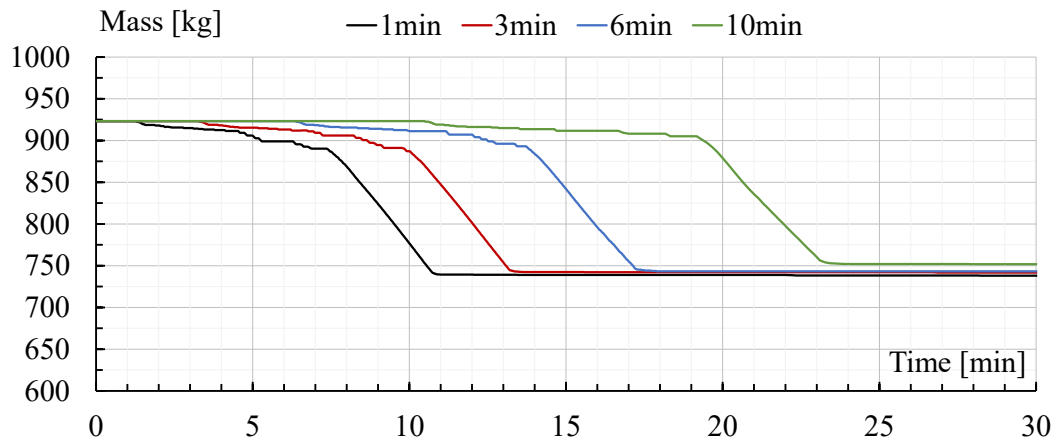


Figure 15. Secondary loop water mass inventory trend with different MHX isolation times

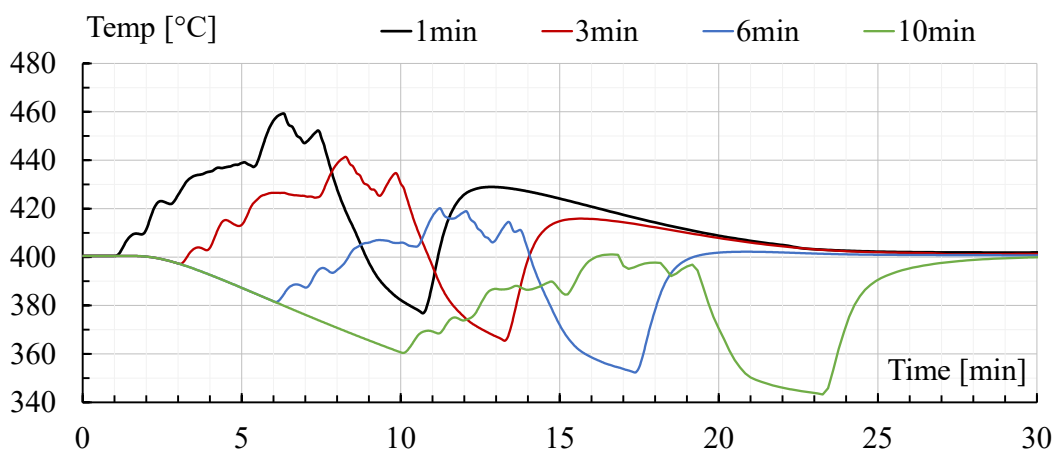


Figure 16. Lead temperature trend with different MHX isolation times

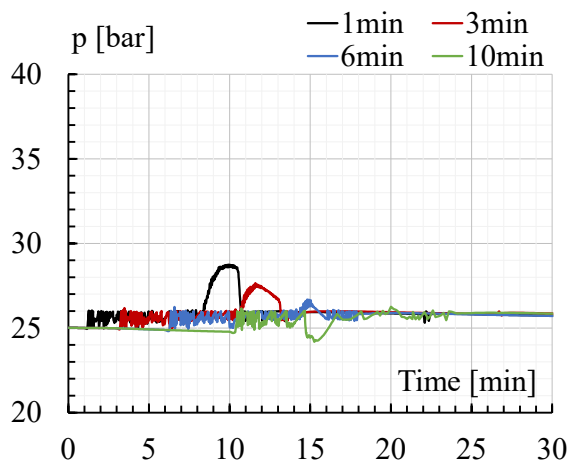


Figure 17. Pressure trend in the PRZ with different MHX isolation time

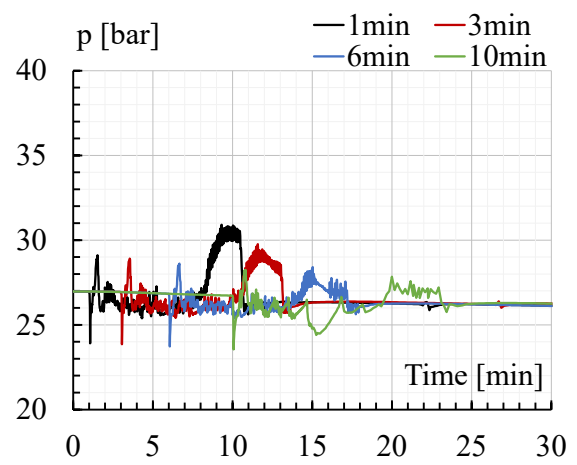


Figure 18. Pressure trend in the MHX with different MHX isolation time

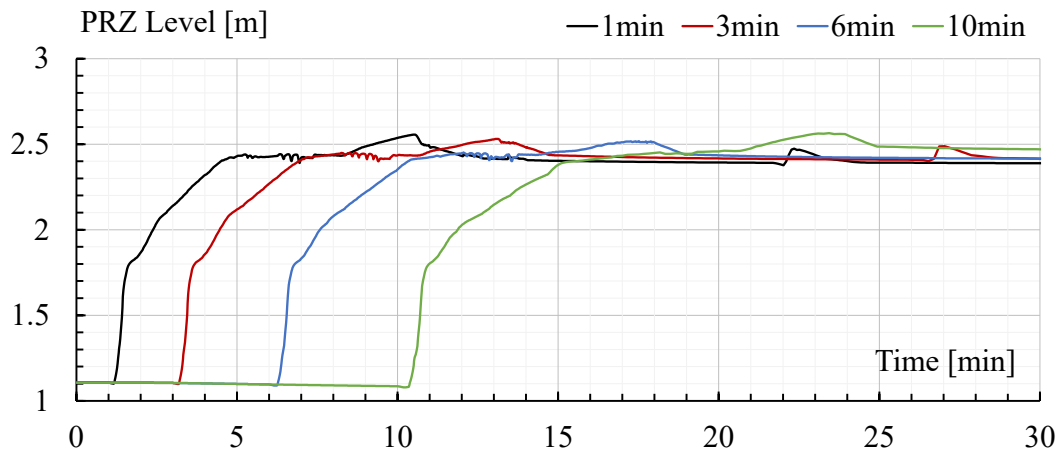


Figure 19. PRZ level at different MHX isolation times

III.C.2. Sensitivity analysis on the CS shutdown time

Considering the cases in which the MHX is isolated from the secondary loop at 1 and 3 minutes only, a further sensitivity analysis has been carried out decreasing the shutdown time of the CS. In this way, the energy released in this phase to the lead is lower, and the MHX can be isolated in a shorter time.

Figures 20 and 21 show that decreasing the shutdown time, lead temperature decreases faster, and the minimum temperature (reached at the closure of the PRZ discharge valve) is lower. If the MHX is isolated after 3 minutes, the lead temperature rise at the MHX outlet is smoother. Anyway, Figure 22 shows that the CS inlet temperature is not affected by the shutdown time since the huge lead inventory in the cold pool results in significant thermal inertia of the primary system.

All the other quantities are not affected by the CS shutdown time except for the pressure in the secondary loop, whose peak is higher if the CS power is decreased slowly because of the higher amount of energy delivered to the fluid. However, Figure 23 to Figure 26 show that the peak is below the limit which could compromise the integrity of the components.

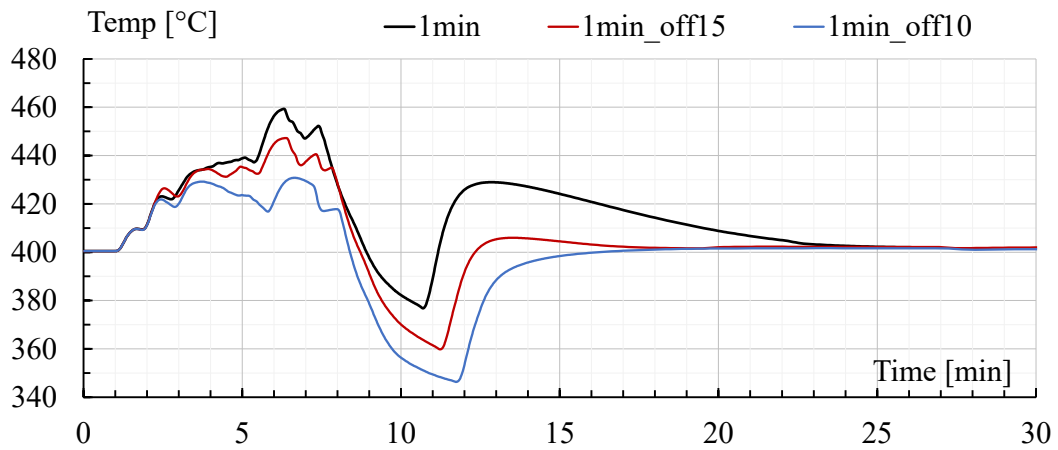


Figure 20. Lead temperature trend with different shutdown times and MHX isolated after 1 minute

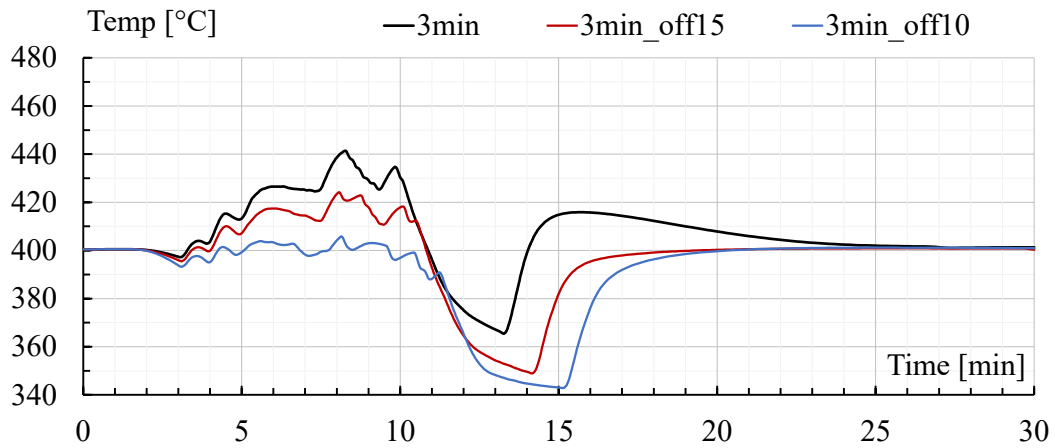


Figure 21. Lead temperature trend with different shutdown times and MHX isolated after 3 minutes

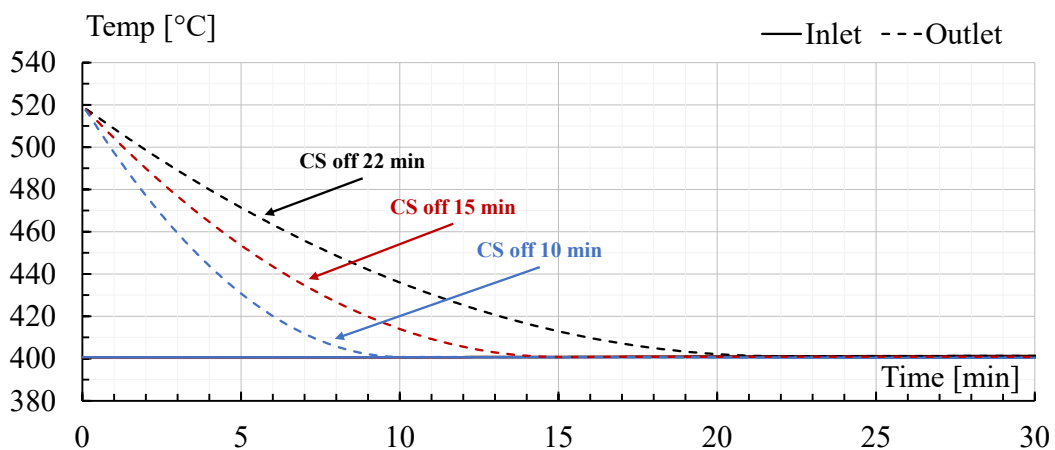


Figure 22. Lead temperature at CS inlet and outlet for different shutdown times and MHX isolated after 1 minute

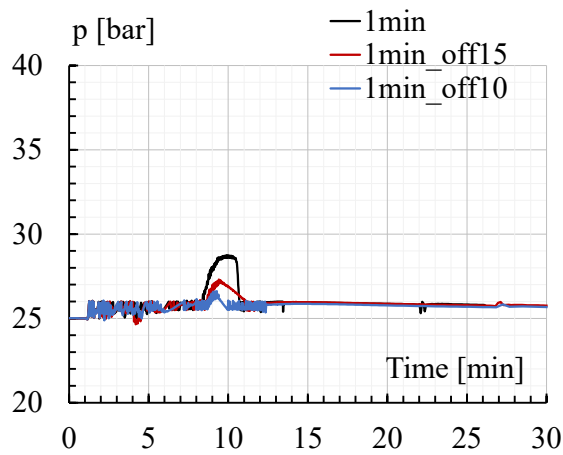


Figure 23. PRZ pressure trend with different shutdown time and MHX isolated after 1 minute

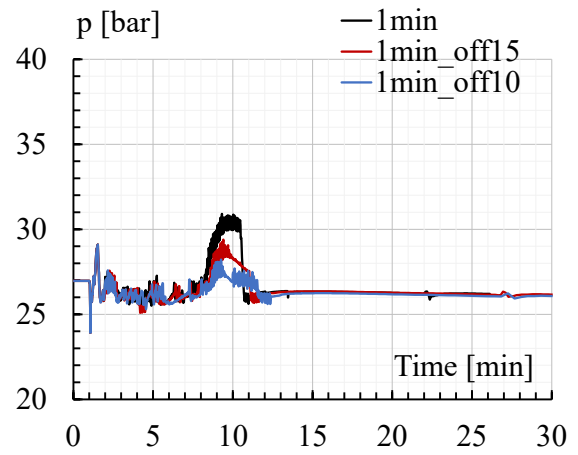


Figure 24. MHX pressure trend with different shutdown time and MHX isolated after 1 minute

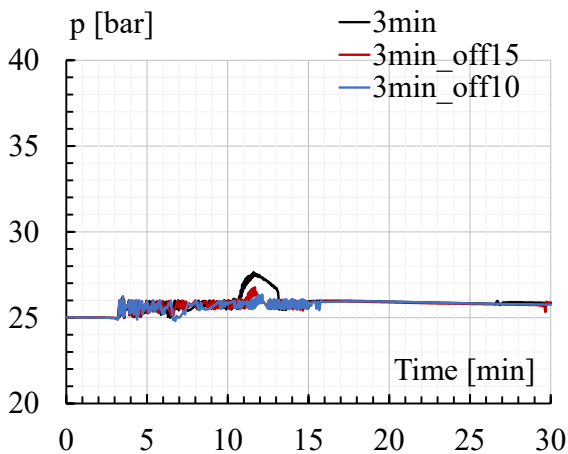


Figure 25. PRZ pressure trend with different shutdown time and MHX isolated after 3 minutes

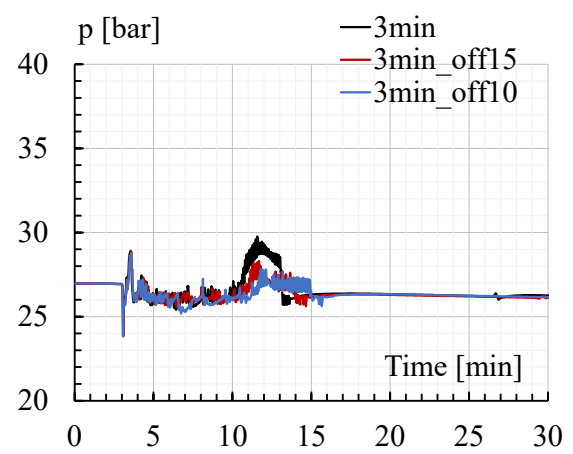


Figure 26. MHX pressure trend with different shutdown time and MHX isolated after 3 minutes

IV. CONCLUSIONS

In the framework of the R&D activities in support of ALFRED project, ATHENA is one of the facilities identified to perform integral tests on components on a relevant scale for Gen-IV Nuclear Reactor related technologies. ATHENA experimental facility has been described focusing on the main components of the pool and of the secondary loop, along with the numerical model of the primary and secondary systems realized through the system thermal-hydraulic code RELAP5/Mod3.3. Following the staged

approach foreseen for ALFRED reactor, ATHENA experimental facility will be operated in conditions representative of Stage 2 and Stage 3. In this paper, Stage 3 conditions have been presented.

After a thermal-hydraulic steady state characterization of the facility, the shutdown transient has been analyzed, during which the CS is switched off in 22 minutes and the MHX is intercepted after few minutes to disconnect the heat sink. The thermal-hydraulic analysis of the shutdown phase is important for the definition of the control logics to be implemented in the control system for the facility operation. The transient develops as follows:

1. while the CS reduces the power delivered to the lead, water flowing in the MHX continues to remove power. During this phase lead temperature decreases because of the high heat transfer coefficient of the water;
2. after few seconds from the closure of the MHX isolation valves and the opening of the venting line valve, water in the BTs of the MHX quickly boils off because of the small water mass inventory, i.e., thermal inertia. During this phase the lead temperature at the MHX outlet increases because the steam is not able to remove power due to its very low heat transfer coefficient compared to liquid water;
3. the steam produced in the MHX goes directly to the PRZ where it is suppressed until the water in the PRZ reaches saturation conditions, and it is not able anymore to condense steam coming from the MHX. At this moment (~7 min from the isolation valves closure) the PRZ discharge valve de-pressurize the component by discharging steam/water from the top of the PRZ. During this phase (at ~4 min), the liquid water remained

trapped in the feedwater collector of the MHX flows inside the BTs cooling the lead, boiling, and then going to the PRZ;

4. at the end of the transient, lead temperature stabilizes at 400°C in the whole pool, and only few kilograms of steam remains in the MHX which is isolated from the secondary loop through the interception valves.

The main results of the sensitivity analysis on the MHX isolation time (1, 3, 6, and 10 minutes) can be summarized as follows:

- fixed the CS shutdown time, the later is the MHX isolation the lower is the minimum temperature of the lead at the MHX outlet because of the high capability of liquid water to remove heat;
- the trends of the main quantities are the same for all the cases, but the curves are translated compared to each other depending on the MHX isolation time. Pressure peaks magnitude in the PRZ and the MHX also depend on the isolation time: the later is the isolation, the lower is the peak.

To avoid the decreasing too much of the lead temperature, it is favorable to isolate the MHX in 1-3 minutes, since pressure peaks remain below the design pressure of the secondary side components (4 MPa). Results of the sensitivity analysis on the shutdown time (22, 15, and 10 minutes) can be summarized as follows:

- decreasing the shutdown time, the lead temperature at the MHX outlet increases slower because of the lower energy released from the CS during the shutdown phase;
- pressure peaks in the PRZ and the MHX are lower in the 3 min case, but lead temperature decreases too much if the CS is shut down in less than 22 min.

The numerical analysis presented in this paper will be the basis to define the operational procedures of the plant, providing preliminary feedback to the operator about the control logics to be implemented in the control system of the facility.

References

- [1] P. LORUSSO et al., “Gen-IV LFR Development; Status & Perspectives”, *Progress in Nuclear Energy*, 105, 318 (2018); <https://doi.org/10.1016/j.pnucene.2018.02.005>.
- [2] Gen IV International Forum (2020), “Generation IV Goals”; https://www.gen-4.org/gif/jcms/c_9502/generation-iv-goals
- [3] J. PACIO et al., “Advanced Thermal-Hydraulic experiments and instrumentation for heavy liquid metal reactors”, *Nuclear Engineering and Design*, 399, 112010 (2022); <https://doi.org/10.1016/j.nucengdes.2022.112010>.
- [4] A. ALEMBERTI et al., “ALFRED and the lead technology research infrastructure”, *Proceedings of European Research Reactor Conference (RRFM)* (2015).
- [5] M. FRIGNANI et al., “ALFRED: A Strategic Vision for LFR Deployment”, *ANS Winter Meeting 2017*, Washington, D.C., October 29-November 2, 2017.
- [6] M. FRIGNANI et al., “FALCON advancements towards the implementation of the ALFRED Project”, IAEA-CN245-485.
- [7] M. FRIGNANI, A. ALEMBERTI and M. TARANTINO, “ALFRED: A revised concept to improve pool related thermal-hydraulics”, *Nuclear Engineering and Design*, 355, 110359 (2019); <https://doi.org/10.1016/j.nucengdes.2019.110359>.
- [8] M. CONSTANTIN et al., “The development of the research infrastructure in support of ALFRED demonstrator implementation in Romania”, *EMERG – Energy. Environment. Efficiency. Resources. Globalization*, 7, 1 (2021), pp. 123-132; <http://dx.doi.org/10.37410/EMERG.2021.1.10>
- [9] K. UMMINGER and A. DEL NEVO, “Integral Test Facilities and Thermal-Hydraulic System Codes in Nuclear Safety Analysis”, *Science and Technology of Nuclear Installations*, 2012, 826732, pp. 1-3 (2012); <https://doi.org/10.1155/2012/826732>
- [10] International Atomic Energy Agency, “Safety Assessment for Facilities and Activities”, pp. 26, IAEA, Vienna (2016).
- [11] M. TARANTINO et al., “Overview on Lead-Cooled Fast Reactor Design and Related Technologies Development in ENEA”, *Energies* 2021, 14, 5157; <https://doi.org/10.3390/en14165157>.
- [12] Information System Laboratories, “RELAP5/Mod3.3 code manual volume I: code structure, system models, and solution methods”, July 2003
- [13] Information System Laboratories, “RELAP5/Mod3.3 code manual volume II: user’s guide and input requirements”, January 2003
- [14] Information System Laboratories, “RELAP5/Mod3.3 code manual volume II: appendix A input requirements”, June 2004
- [15] Information System Laboratories, “RELAP5/Mod3.3 code manual volume VII: summaries and reviews of independent code assessment reports”, December 2001
- [16] Information System Laboratories, “RELAP5/Mod3.3 code manual volume V: user’s guidelines”
- [17] M. FRIGNANI et al., “ALFRED staged approach”, *Proceedings of the ICAPP 2019 Conference* (2019)
- [18] M. TARANTINO et al., “Integral Circulation Experiment: Thermal-hydraulic simulator of a heavy liquid metal reactor”, *Journal of Nuclear Materials*, 415, 3, 433, (2011); <https://doi.org/10.1016/j.jnucmat.2011.04.033>.
- [19] P. LORUSSO et al., “Experimental Analysis Of Stationary And Transient Scenarios Of ALFRED Steam Generator Bayonet Tube In CIRCE-HERO Facility”, *Nuclear Engineering and Design*, 352, 110169 (2019); <https://doi.org/10.1016/j.nucengdes.2019.110169>.

- [20] P. LORUSSO et al., “MYRRHA primary heat exchanger experimental simulations on CIRCE-HERO,” *Nuclear Engineering and Design*, 353, 110270 (2019); <https://doi.org/10.1016/j.nucengdes.2019.110270>.
- [21] P. LORUSSO, A. PESETTI and M. TARANTINO, “ALFRED Steam Generator Assessment: design and pre-test analysis of HERO experiment”, *Proceedings of the 2018 26th International Conference on Nuclear Engineering*, July 22-26, 2018, London, England, ICONE26-81824; DOI: [10.1115/ICONE26-81824](https://doi.org/10.1115/ICONE26-81824).
- [22] P. LORUSSO et al., “Design of a novel test section for the LFR development: the CIRCE-THETIS facility”, *28th International Conference on Nuclear Engineering (ICONE28)*, August 4-6, 2021, virtual conference, Volume 2, Article number V002T07A032; DOI: [10.1115/ICONE28-65575](https://doi.org/10.1115/ICONE28-65575)
- [23] M. TARANTINO et al., “Preliminary design of a helical coil steam generator mock-up for the CIRCE facility for the development of DEMO LiPb heat exchanger”, *Fusion Engineering and Design*, 169, 112459 (2021); <https://doi.org/10.1016/j.fusengdes.2021.112459>.
- [24] T. DEL MORO, P. CIOLI PUVIANI, “ATHENA main flow path analysis”, AT-D-R-621, Rev. 0, ENEA Report (June 2022).
- [25] R. MARINARI, I. DI PIAZZA, “Technical specification of the ATHENA main circulation pump”, AT-D-S-608, Rev. 3, ENEA Report (Aug. 2022).
- [26] T. DEL MORO et al., “ATHENA main heat exchanger conceptual design and thermal-hydraulic assessment with RELAP5 code”, *29th International Conference on Nuclear Engineering (ICONE29)*, August 8-12, 2022, Virtual, ICONE29-91997; <https://doi.org/10.1115/ICONE29-91997>
- [27] P. CIOLI PUVIANI, “ATHENA dead volume thermo-fluid dynamics design”, AT-N-R-578, Rev. 0, ENEA Report (Jan. 2022).
- [28] V. NARCISI, F. GIANNETTI and G. CARUSO, “Investigation on RELAP5-3D[®] capability to predict thermal stratification in liquid metal pool-type system and comparison with experimental data”, *Nuclear Engineering and Design*, 352, 110152 (2019); <https://doi.org/10.1016/j.nucengdes.2019.110152>
- [29] P. LORUSSO et al., “Total Loss of Flow Benchmark in CIRCE-HERO integral test facility”, *Nuclear Engineering and Design*, 376, 111086 (2021); <https://doi.org/10.1016/j.nucengdes.2021.111086>.
- [30] V. NARCISI et al., “Post-test simulation of a PLOFA transient test in the CIRCE-HERO facility”, *Nuclear Engineering and Design*, 355, 110321 (2019); <https://doi.org/10.1016/j.nucengdes.2019.110321>
- [31] OECD/NEA Nuclear Science Committee, *Handbook on Lead-bismuth Eutectic Alloy and Lead Properties*, Materials Compatibility, edition, Thermal-hydraulics and Technologies (2015)
- [32] M. TARANTINO et al., “Post Test Analysis of ICE Tests”, *Proc. of 20th Int. Conf. on Nuc. Eng. (ICONE20)*, Anaheim, CA, USA, July 30–August 3, 2012, Paper No. ICONE20-54952, Vol. 2, pp. 703-712, 10 pages.
- [33] E. MARTELLI et al., “Thermal hydraulic modeling and analyses of the water-cooled EU DEMO using RELAP5 system code”, *Fusion Engineering and Design*, (2019); DOI: [10.1016/j.fusengdes.2019.02.021](https://doi.org/10.1016/j.fusengdes.2019.02.021).
- [34] N. FORGIONE et al., “Post-test simulations for the NACIE-UP benchmark by STH codes”, *Nuclear Engineering and Design*, 353, 110279 (2019); <https://doi.org/10.1016/j.nucengdes.2019.110279>.
- [35] P. CIOLI PUVIANI, “ATHENA Core Simulator. Thermo-fluid dynamics design”, AT-N-R-597, Rev. 0, ENEA Report (Mar. 2022).

Nomenclature

Acronyms

AC	Air Cooler
ALFRED	Advanced Lead-cooled Fast Reactor European Demonstrator
ATHENA	Advanced Thermal-Hydraulic Experiment for Nuclear Applications
BT	Bayonet Tube
BWG	Birmingham Wire Gauge
CIRCE	CIRColazione Eutettico (Eutectic Circulation)
CFD	Computational Fluid Dynamics
CS	Core Simulator
EC	European Commission
ENEA	Agenzia nazionale per le nuove tecnologie, l'energia e lo sviluppo economico sostenibile
FA	Fuel Assembly
FALCON	Fostering ALfred CONstruction
FC	Feeding Conduit
Gen-IV	Generation-IV
HERO	Heavy liquid mEtal pRessurized water cOoled tubes
HLM	Heavy Liquid Metal
ID	Inner Diameter
LFR	Lead-cooled Fast Reactor
MCP	Main Circulation Pump
MHX	Main Heat eXchanger
OD	Outer Diameter
P&ID	Piping and Instrumentation Diagram
PRZ	PressuRiZer
RATEN ICN	Regia Autonoma Tehnologii pentru Energia Nucleara – Institutul de Cercetari Nucleare
RELAP	Reactor Excursion and Leak Analysis Program
R&D	Research & Development
Sch.	Schedule
SoT	Start of Transient
STH	System Thermal-Hydraulic
THETIS	Thermal-hydraulic HELical Tubes Innovative System
TMDPJUN	TiMe-DePendent JUNction
TMDPVOL	TiMe-DePendent VOLume

Alphabetical symbols

p	pressure, Pa
T	temperature, K

Greek symbols

Γ	mass flow rate, kg/s
Δ	difference

Subscripts

Cen.A.	Central Assembly
Ext.A.	External Assemblies
in	inlet
out	outlet
TOT	TOTal